

# FAILURE ANALYSIS OF COMPOSITE BOLTED JOINTS BY AN EXPERIMENTAL AND A NUMERICAL APPROACH

B. Montagne<sup>1</sup>, F. Lachaud<sup>1</sup>, E. Paroissien<sup>1</sup> and D. Martini<sup>2</sup>

<sup>1</sup>Institut Clément Ader (ICA), Université de Toulouse, CNRS, INSA, ISAE-SUPAERO, Mines Albi, UPS, 3 rue Caroline Aigle 31400 Toulouse, France

Email: [benoit.montagne@isae.fr](mailto:benoit.montagne@isae.fr) , [frederic.lachaud@isae.fr](mailto:frederic.lachaud@isae.fr) , [eric.paroissien@isae.fr](mailto:eric.paroissien@isae.fr)

<sup>2</sup>Dassault Aviation, 78 Quai Marcel Dassault 92210 Saint-Cloud, France

Email: [dominique.martini@dassault-aviation.com](mailto:dominique.martini@dassault-aviation.com)

**Keywords:** Composite material, bolted joint, finite element analysis

## Abstract

Composite materials are widely used by aircraft manufacturers because of their high mechanical properties. These properties severely decrease when composite material are drilled and bolted. To avoid structural failure, the behavior of composite bolted joints has to be understood and mastered. An experimental database was constituted by Dassault Aviation with supported single-shear tests with countersunk head screws on different composite materials. This database is analysed to find the main parameters that lead to the failure of the joint. The end distance is the most important parameter. It has a strong influence on both the bearing stress at failure and the failure mode. Width and lay-up have a lower effect on joint failure. A two-dimensional finite element (FEM) model with elastic membrane behavior is then developed to simulate the different configurations in the database. Fiber failure criteria is computed and the dispersion of the results for each failure mode is compared to the dispersion of the experimental data to evaluate the quality of the model. The modification of the failure criteria by taking into account different ply orientations and shear stress permits to reduce the dispersion but it is still higher than the dispersion of the experimental data. This work highlights the limits of such linear 2D modelling and it confirms the needs for more complex modelling such as the local bending effects of the joints and/or the non linear behavior of the composite material.

## 1. Introduction

Aeronautical structures are made with a lot of pieces assembled together. These joints are mainly done with bolts or rivets. Bolted or riveted joints are easier to tear down than welding or bonding. It permits low cost maintenance operations. Dassault Aviation's aircrafts count hundreds of thousands of fasteners (250 000 on the Falcon 7X and 300 000 on the Rafale). This number could raise to a few millions on the biggest planes such as civil airliners. Nowadays, composite materials are more and more used by aircraft manufacturers. To satisfy the current performance and safety aircraft requirements, it is therefore necessary to master the composite bolted joints behavior. However these joints are difficult to model because of contact and geometrical or material non linearity issues. In a joint, the bolts transfer the load to the different parts. It results in mechanical degradations in the composite material, what could lead to different failure modes of the structure depending on the design parameters such as geometry or lay-up. Therefore, aircraft manufacturers have to understand these modes in order to optimize their design.

In this context Dassault Aviation in collaboration with Institut Clément Ader has started a research project to study composite bolted joint behavior and its modelling. The goal of this project is to define the necessary modelling complexity for characterizing the effects of these design parameters on the

failure modes of composite bolted joints. This subject has been studied for many years. Hart-Smith [1-3] developed a phenomenological approach that resulted in design rules for composites bolted joints. Analytical method based on electrical analogy proposed by Ross [4] lead to several stiffness formulas [5-8] that often need to be adjusted to fit experimental data. Finite element method is another way to study bolted joints. In this paper, an analysis of the experimental database on composite bolted joints provided by Dassault Aviation is presented first for identifying the most important design parameters regarding to bolted joint strength. A two-dimensional FEM is then developed on Samcef v18.1 for improving the understanding of the design parameter influence on the failure of composite bolted joints. This modelling allows an accurate description of the geometry (diameter, width and end distance), the lay-up and the bolt/hole contact. At this point, the composite material behavior is assumed to be elastic and orthotropic.

## 2. Experimental results and database analysis

The present database was generated by Dassault Aviation during several experimental studies on composite bolted joints. This database consists in supported single-shear specimens with countersunk head screw with different materials, lays-up, widths and end distances. The specimens are made of composite material jointed with aluminium plates. The countersunk screw head is located in the composite part. In the following analysis the failure stress corresponds to the bearing stress when the specimen load is maximum. The failure modes observed for the different configurations were sorted following the usual classification [1] which is presented in Fig. 2. These failure modes are influenced by design parameters such as the end distance ( $P$ ), the width ( $2D$ ) or the lay-up.

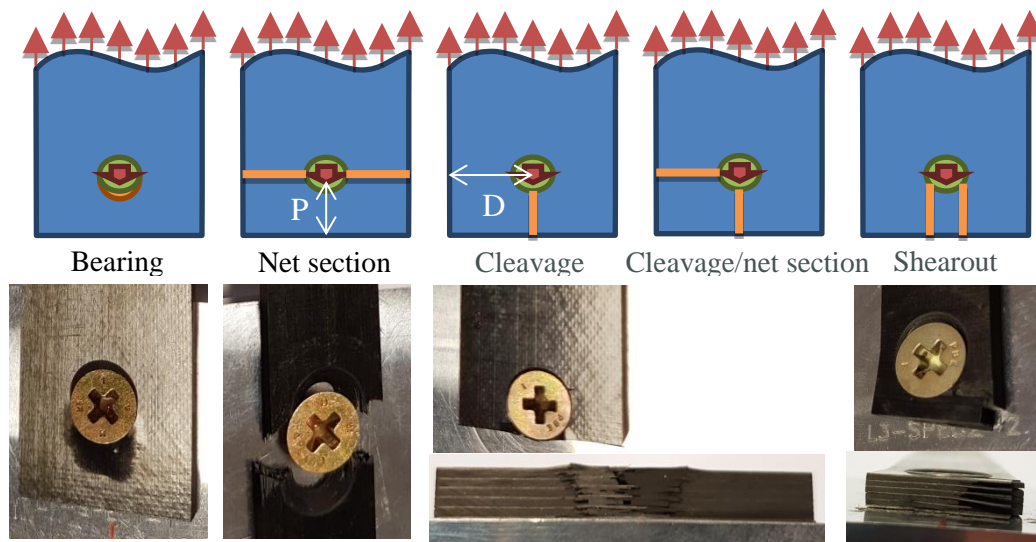


**Figure 2.** Failure modes of composite bolted joints

### 2.1. Influence of the end distance

The bearing stresses at failure are plotted with respect to the end distance  $P$  divided by the hole diameter  $\phi$  in Fig. 3. Three different T700GC/M21 laminates are studied here. Their proportions of plies oriented in the 4 directions are presented in the following way:  $0^\circ/45^\circ/-45^\circ/90^\circ$ . The shape of the points indicates the failure mode and its color the laminate. The graphs presented in this paper are normalized.

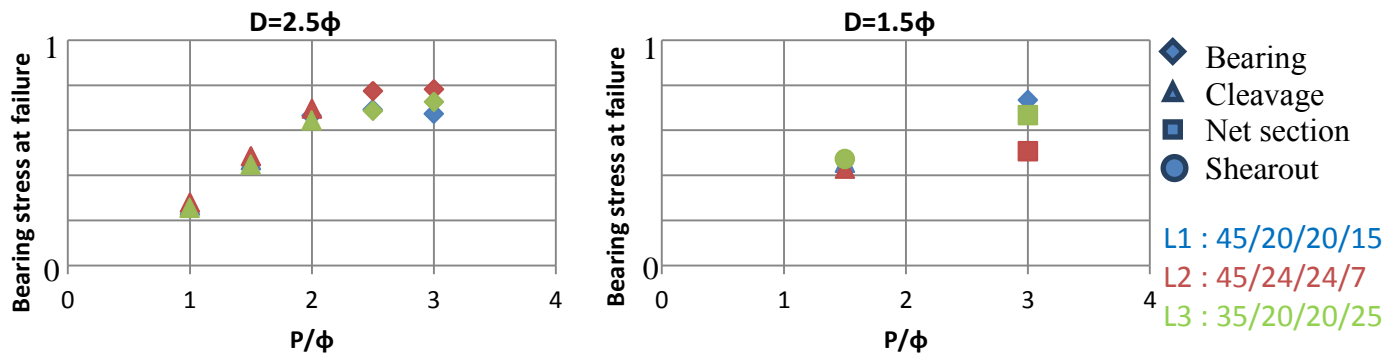


**Figure 3.** Bearing stresses at failure with respect to the edge distance

From Figure 3, we observe that specimens fail in bearing mode at a relatively constant stress when the end distance  $P$  is large enough ( $> 2\phi$ ). When  $P$  decreases ( $\phi \leq P \leq 2\phi$ ) the cleavage failure mode is observed with a failure stress reduction. This reduction is proportional to  $P$ . These results were also observed by Collings [9] and are coherent with industrial criteria. Hart-Smith [3] also observed constant failure stresses for the bearing failure of T300/N5208 double shear specimens with large  $P$ .

It is indicated that if the end distance is large enough ( $P=3\phi$ ) for avoiding cleavage failure mode, the net section failure mode could then be observed when  $D$  is small as illustrated in figure 3. Hart-Smith [1-3] advised to use laminates with a repartition of plies in the four directions ( $0^\circ, 45^\circ, -45^\circ$  and  $90^\circ$ ) between  $1/8$  (12.5%) and  $3/8$  (37.5%) within the laminates in order to favor bearing failure. The three laminates studied here have the following repartitions of  $90^\circ$ -oriented plies:

- L1 = 45%/20%/20%/15%
- L2 = 45%/24%/24%/7%
- L3 = 35%/20%/20%/25%

The failure modes of these laminates agree with this design rule: the net section failure mode of L2 laminate leads to a significant reduction in the failure bearing stress compared to the bearing failure mode when it does not for L3 laminate.

Lastly, when the end distance is reduced ( $\phi \leq P \leq 2\phi$ ), the variation of the failure bearing stresses of the three laminates is reduced compared to this same variation when  $2.5\phi \leq P \leq 3\phi$  even if different failure modes are observed when  $P \leq 2\phi$ . The pictures on Figure 4 illustrate these different failure modes showing the end edge of the failed specimens (L1 and L2 cleavage and L3 shearout) when  $P=1.5\phi$ . The L1 and L2 specimens present a straight failure behind the bolt which is specific to cleavage. The  $90^\circ$  plies of the L3 specimen are strongly delaminated thus they are not within the laminates anymore.

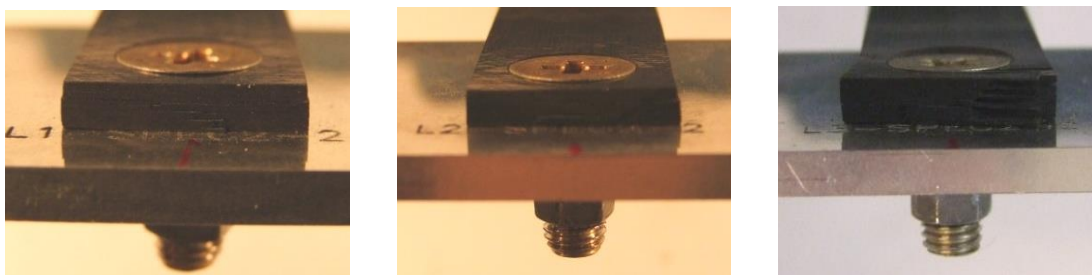


**Figure 4.** Post-failure specimens that failed in cleavage and shear-out (from left to right: L1, L2 and L3)

## 2.2. Influence of the width

The Figure 5 shows the evolution of the failure bearing stresses as a function of D ( $W=2D$ ) for two values of P. This D parameter does not seem to have a significant effect on stresses at failure except for the net section failure mode of the L2 laminate as mentioned before. Modifying D does not change the failure mode when the end distance is short ( $P=1.5\phi$ ) even if the L3 laminates failed by shearout. When the end distance is larger ( $P=3\phi$ ) the reduction of D leads to net section failures but the failure bearing stresses are almost unchanged for well proportioned laminates.

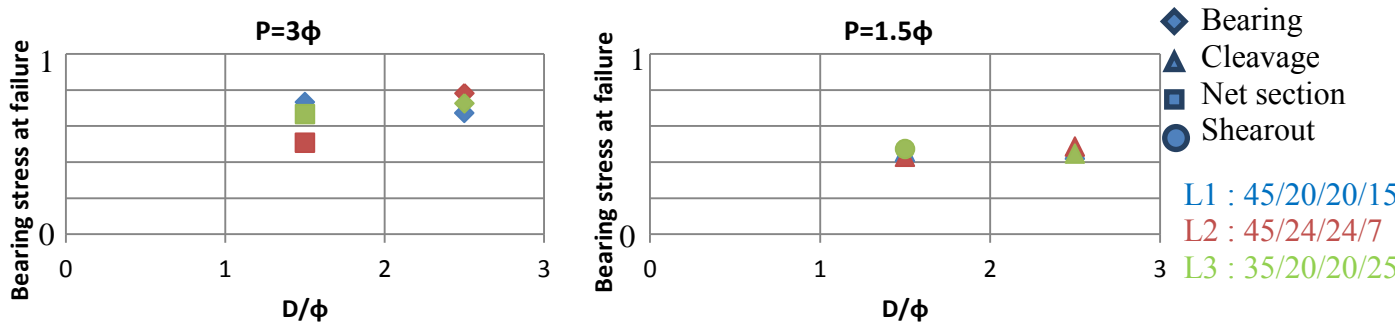


Figure 5. Bearing stress at failure with respect to D ( $W=2D$ )

## 2.3. Influence of the load orientation

The geometrical parameters are set to  $P=3\phi$  and  $D=2.5\phi$  for analysing the influence of the load orientation (i.e. the angle between the  $0^\circ$  plies and the direction of loading). In this part, the studied specimens are made in T800S/M21 with two different 50/20/20/10 stacking sequences. According to the Fig. 6 there is no effect of the load orientation on the failure bearing stresses or on the failure mode (bearing) excepted for the  $90^\circ$  angle. In this case, the failure mode is net section for a slightly smaller stress at failure ( $\sim 10\%$  drop compared to the  $0^\circ$  angle).

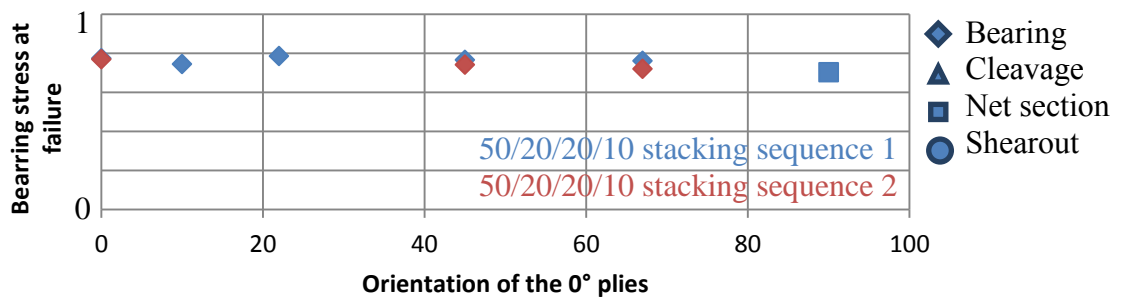


Figure 6. Bearing stress at failure according to the angle between the  $0^\circ$  plies and the loading direction

## 2.4. Conclusions

From experimental data analysis we conclude that the most influent design parameter on the joint strength is the end distance P. It has a strong effect on the failure modes and stresses. The D parameter and the loading direction only have a second order influence on bolted joints strength. The same results are obtained for IMS/977-2 and T800S/M21 materials. This conclusion is also in agreement with Hart-Smith's observations [1-3] on other composite materials and should be therefore a intrinsic characteristics of composite materials bolted joints.

### 3. Two-dimensional finite element analysis

A two-dimensional FEM is then developed for improving the comprehension of the effect of the design parameter on the joint strength. This modelling allows a precise description of the geometry of the previously presented joint configurations and therefore of the associated strain and stress fields in the hole neighbourhood. A first-ply failure analysis is then performed using the Hashin's failure criteria for predicting the different failure modes presented in this work. The failure of the laminate is expected when at least one of its plies failed. The objective is to reduce the dispersion of the experimental results compared to the previous failure bearing stress analysis. The dispersion is characterized by the coefficient of variation (CoV) which is the standard deviation divided by the mean of the considered values

#### 3.1. Model presentation

The FEM is developed on Samcef Software (SIEMENS PLM Software). The configurations are the previously mentioned ones (i.e. T700GC/M21, IMS 977-2 and T800S/M21 materials with different sets of P, D and lays-up). The materials of the finite element model are linear and elastic. The T700GC/M21 mechanical properties are listed in the Table 1. The Young modulus and stresses at failure for IMS977-2 and T800S/M21 are 10% higher than these ones.

**Table 1.** Mechanical properties of the T700GC/M21 UD ply.

$E_{11}$	$E_{22} = E_{33}$	$G_{12} = G_{13}$	$G_{23}$	$\nu_{12} = \nu_{13}$	$\nu_{23}$	$\sigma_{11}^{RT}$	$\sigma_{11}^{RC}$	$\sigma_{22}^{RT} = \sigma_{33}^{RT}$	$\sigma_{22}^{RC} = \sigma_{33}^{RC}$	$\sigma_{12}^R = \sigma_{13}^R$	$\sigma_{23}^R$
135000	8500	4800	3200	0.31	0.42	2300	1450	70	300	95	60

The bolt is modelled by a steel disk (isotropic linear elastic material). A drawing of the model is presented Fig. 7. The prescribed force  $F$  is equal to the experimental maximum force applied during the test thus it varies for each configuration. The center of the bolt is fixed and node to node contact elements are used for modeling the contact between the disk and the composite plate. A nominal clearance is also introduced between the bolt and the hole and soft springs are used to avoid rigid body modes. Lastly, composite membrane elements with two degrees of freedom (displacement) are used to model the plate and to get the strain and stress fields in each ply of the laminate.

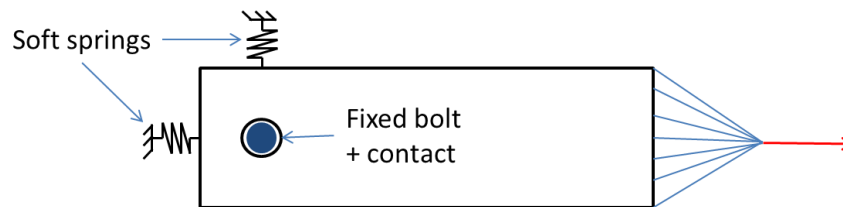


**Figure 7.** Boundary conditions of the 2D FE model

#### 3.2. Results

All the configurations in the experimental database were computed with the 2D FEM. The Figure 8 shows the fiber strains for three of the four plies orientation ( $0^\circ$ ,  $45^\circ$  and  $90^\circ$ ).

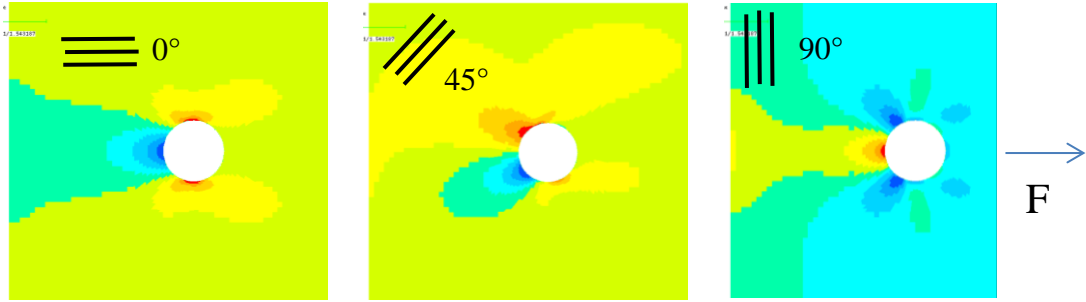


**Figure 8.**  $\epsilon_{FF}$  in the different plies orientation (here  $P=3\phi$  and  $D=2.5\phi$  )

These fiber strains are in compression (blue zones on Fig. 8) where the fiber directions are normal to the hole edge. They are in tension (red zones on Fig. 8) where the fiber directions are tangent to the hole edge. Assuming a first-ply failure, the Hashin's criteria could be set in the different plies according to the expected failure modes. Hashin's criteria [10] is presented in Table 2. In this analysis, we only consider the fiber failure criteria.

**Table 2.** Hashin criteria

Hashin criteria	Tension	Compression
Fibers	$\left(\frac{\sigma_{11}}{\sigma_{11}^{RT}}\right)^2 + \frac{\sigma_{12}^2 + \sigma_{13}^2}{\sigma_{12}^R{}^2}$	$\left(\frac{\sigma_{11}}{\sigma_{11}^{RC}}\right)^2$
Matrix	$\frac{(\sigma_{22} + \sigma_{33})^2}{\sigma_{22}^{RT}{}^2} + \frac{\sigma_{23}^2 - \sigma_{22}\sigma_{33}}{\sigma_{23}^R{}^2} + \frac{\sigma_{12}^2 + \sigma_{13}^2}{\sigma_{12}^R{}^2}$	$\left(\left(\frac{Y_C}{2\sigma_{23}}\right)^2 - 1\right)\left(\frac{\sigma_{22} + \sigma_{33}}{\sigma_{22}^{RC}}\right) + \left(\frac{\sigma_{22} + \sigma_{33}}{2\sigma_{22}^{RC}}\right)^2 + \frac{\sigma_{23}^2 - \sigma_{22}\sigma_{33}}{\sigma_{23}^R{}^2} + \frac{\sigma_{12}^2 + \sigma_{13}^2}{\sigma_{12}^R{}^2}$

The values of the stress at failure are reported in Table 1. For bearing failure analysis, the Hashin criterion for fiber failure in compression is used for the  $0^\circ$  and  $\pm 45^\circ$  plies. For cleavage failure mode, the tension fiber criterion in  $90^\circ$  plies is used. Finally, for net section failure mode, the tension fiber criterion is analysed in the  $0^\circ$  plies. A maxima stress criterion in fiber direction is also computed to study the influence of shear in the Hashin's criteria. Its expression is presented in Eq. 1 (T:Tension and C : Compression).

$$\frac{\sigma_{11}^{RT/C}}{\chi^{T/C}} \leq 1 \quad (1)$$

### 3.2.1. Cleavage

The cleavage appears when the end distance is strictly smaller than  $2,5\phi$ . The Figure 9 shows the results obtained for the maximal stress and Hashin's criteria for tension fiber failure in  $90^\circ$  plies.

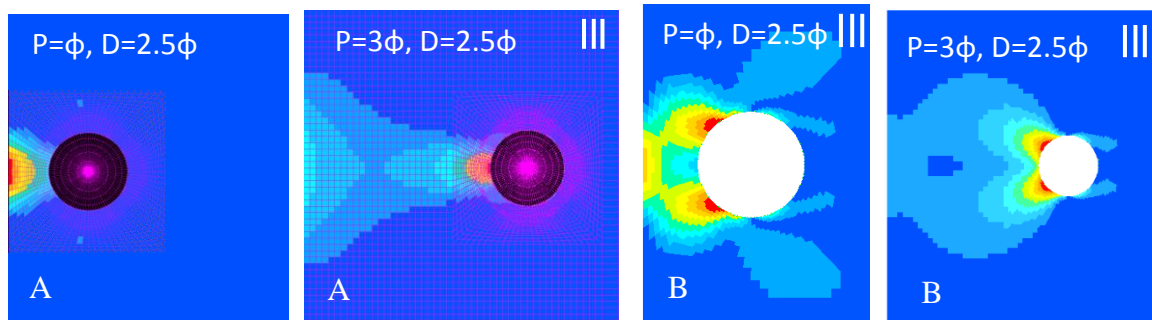


**Figure 9.** Maximal stress criterion (A) with short and large end distance and Hashin's criterion (B) with short and large end distance for tension fiber failure in 90° plies

Both criteria maximum values are smaller than 1 thus they do not predict the cleavage failure of the specimens. When the edge distance  $P$  is large, it is obvious since the experimentally observed failure is bearing. Nevertheless, this result is the same when  $P$  reduces. Moreover, the maximum criterion locations are different between maximum and Hashin's criteria: the Hashin's criterion is maximum where shear stress is maximum, at 40° from the load orientation, when the maximum stress criterion is maximum at 0° as illustrated in Fig. 9. Consequently, Hashin's criterion may over-estimate matrix failure influence on fiber failure. Eleven configurations of T700GC/M21 failed in cleavage. The maximum stress criterion gives an average of half the Hashin's criterion average. Their CoV are of 21% for the maximum stress criterion and of 18% for the Hashin's criterion while the experimental data CoV is 8.8% assuming a linear evolution of the failure bearing stress as a function of  $P$ . Both of the criteria give worse dispersions than the experimental one.

### 3.2.2. Net section

Only three specimens of T700GC/M21 have failed in net section in the database. Both maximum stress and Hashin's fiber failure criteria were computed in the 0° plies. They respectively give 36% and 28% CoVs while the CoV of the experimental data equals 14% assuming a constant net stress at failure. Finally, these two criteria gives worse dispersions than the experimental data.

### 3.2.3. Bearing

Bearing is a complex failure mode including several phenomena such as fiber failure in compression, delamination or matrix damage. The assumption here is that the bearing failure of the specimens occurs when 0° or ±45° plies fail due to fiber compression. The Hashin's criterion for fiber failure in compression is the same as the maximal stress criterion. But, it was shown in literature [11] that shear can significantly reduce compression strength in fiber direction. Thus, a shear dependency was introduced in the Hashin's fiber criterion in compression as it is for tension. The maximal stress criterion gives a CoV of 10% for T700GC/M21 specimens. Let's note that failure mainly occurs in ±45° plies where maximum fiber compression is higher than in 0° plies. This result agrees with Gohorianu's observations [12]. The Hashin's criterion gives a higher average value than the maximum stress criterion and a 7.4% CoV for the same specimens. The first-ply failure is balanced between 0° and ±45° plies depending on the geometries and lays-up. The CoV of the experimental data assuming a constant failure bearing stress is 6.3% so those criteria have worse dispersions than the experimental data. For IMS 977-2, the maximal stress criterion gives a CoV of 5.9% and the Hashin's criterion 7.7% with still the highest average value. For this material the CoV of both criteria are better than the CoV of the experimental data (12%).

#### 4. Conclusions

The experimental database provided by Dassault Aviation was analysed to identify the influence of the design parameters on the failure of composite bolted joints. We observed that the end distance has a strong effect on joint failure mode and strength. The width and the loading direction are second order parameters for joint failure modes and strength. A 2D finite element modelling was then performed for improving the comprehension of the joint failure modes and strength. The different failure modes were predicted by a first-ply failure analysis using maximum stress and Hashin's criteria. We observed that the dispersions of the FE simulations were higher than the experimental data assuming simple macroscopic criteria based on the failure bearing stress. Nevertheless, these simulations emphasized the significant effect of shear on the failure of composite bolted joints. In conclusion, the FE modeling must be improved and failure analysis of composite also. This should be done modeling the secondary bending effect that occurs in supported single-shear specimens (even if small) or introducing a non linear behavior of the composite material. The objective is to improve the simulation of strain and stress field distributions in supported single-shear specimens. The secondary bending illustrates the geometrical non linearities in joint behavior. It introduces out of plane stress in the laminate and thus modifies the stress field within the plate thickness. The non linear behavior of the composite material is related to the damage of its constituents such as fiber kinking, matrix cracks or delaminations. Our objective is to identify the role of each damage on the different failure modes and stresses.

#### 5. Acknowledgement

The authors gratefully acknowledge the French DGAC for financially supporting this study

#### References

- [1] L.J. Hart-Smith. Design and analysis of bolted and riveted joints in fibrous composite structures. *Joining Fiber-Reinforced Plastics*, 227-269, 1987.
- [2] L.J. Hart-Smith. Mechanically fastened joints for advanced composites – Phenomenological considerations and simple analysis. *Fibrous Composites in Structural Design*, 543-574, 1980.
- [3] L.J. Hart-Smith. *Bolted joints in graphite-epoxy composites*. NASA CR-144899, 1976.
- [4] R. Ross. *An electrical computer for the solution of shear-lag and bolted joints problem*. NACA, 1947.
- [5] M.T. Tate and S. Rosenfeld. *Preliminary investigation of the loads carried by individual bolts in bolted joints*. NACA, 1946
- [6] T. Swift. Fracture analysis of stiffened structure, damage tolerance of metallic structures : analysis methods and application. *American Society for Testing and Materials (ASTM)*, 69-107, 1984.
- [7] H. Huth. Influence of fastener flexibility on the prediction of load transfer and fatigue life for multiple row joints. *Fatigue in mechanically fastened composite and metallic joints*, 221-250, 1986.
- [8] E. Paroissien, M. Sartor, J. Huet and F. Lachaud. Analytical Two-Dimensional Model of a Hybrid (Bolted/Bonded) Single-Lap Joint. *Journal of Aircraft*, 44 573-582 2007.
- [9] T. Collings. On the bearing strength of CFRP laminates. *Composites*, 543-570, 1980.
- [10] Z. Hashin. Failure criteria for unidirectional fiber composites. *J. Appl. Mech.*, 47 329-334, 1980.
- [11] B. Budiansky. Compressive failure of fiber composites. *J. Mech. Phys. Solids*, 41 183-211, 1993.
- [12] G. Gohorianu. *Interactions entre les défauts d'usinage et la tenue en matage d'assemblages boulonnés en carbone/epoxy*. Université de Toulouse III – Paul Sabatier, 2008.